Supplementary Data

Stroma-targeted nanomedicine rewires cancer-associated fibroblasts subtypes via CHIP activation in pancreatic ductal adenocarcinoma

Ahmed M.R.H. Mostafa[1,a], Ahmed G. Hemdan[1,2,a], Praneeth R. Kuninty[1,a], Tushar N Satav[1], Maike Spijkerman[1], Ran Li[3,4], David Lagares[5], Franck Assayag[6], Miles Miller[3,4], Jai Prakash[1,7,8,*]

[1]Engineered Therapeutics, Advanced Organ Bioengineering and Therapeutics, Department of Bioengineering Technology, TechMed Centre, University of Twente, Enschede, The Netherlands.

[2] Department of Pharmacology and Toxicology, Faculty of Pharmacy, Assiut University, Egypt.

[3]Department of Radiology, Massachusetts General Hospital and Harvard Medical School, Boston, MA, USA.

[4]Center for Systems Biology, Massachusetts General Hospital Research Institute, Boston, MA, USA.

[5]Center for Immunology and Inflammatory Diseases, Division of Rheumatology, Allergy and Immunology, Massachusetts General Hospital, Harvard Medical School, Boston, MA, USA.

[6]Central animal handling laboratory, TechMed Centre, University of Twente, 7500AE, Enschede, The Netherlands.

[7]ScarTec Therapeutics BV, 7522LW, Enschede, The Netherlands.

[8]Department of Medical BioSciences, Radboud University Medical Centre, Nijmegen, The Netherlands.

[a] Shared authorship

*Corresponding address:

Advanced Bioengineering and Therapeutics

Department of Medical Biosciences

Radboud University Medical Centre

Geert Grooteplein Zuid 10

6525GA, Nijmegen

The Netherlands

T (+31)-633865208

Email: jai.prakash@radboudumc.nl

Supplementary material

Molecular docking analysis

To predict the binding sites of AV3 peptidomimetic with α5β1, we performed molecular docking using the Autodock vina version 1.2.0 default protocol [49]. The AV3 peptidomimetic sequence was drawn using Malvern software and docked with (PDB: 7NLW, without ligand). Auto Dock vina analyses docking simulations, including visualizing conformations, conformational similarity, and interactions between ligands and proteins, as well as the affinity potentials created by Auto Grid, placed with the following dimensions: center_x=270.03, center_y=262.47, center_z=256.54. Docking was performed with energy range = 3, exhaustiveness = 8 to obtain the top 5 best poses with the protein. The ligand-protein interaction images were developed using PyMOL software ver. 2.5.5 (Schrodinger, LLC).

RNA isolation and qPCR

hPSC were seeded in 12 well plate (4 x 10^4 cells/well) in complete medium. The next day, cells were starved, and a day later, cells were treated with human transforming growth factor beta (TGF-β1) (5ng/ml) for 24 h. Then, the cells were lysed, and the total RNA was isolated using Nucleospin RNA isolation kit (Bioké, Netherlands). Then, we synthesized cDNA using iScript™ cDNA Synthesis Kit (BioRad, Netherlands). Finally, PCR reaction was performed using 10 ng for each reaction. The real-time PCR primers (Table 1) for human αSMA (ACTA2), ITGA5 & RPS18 were purchased from Sigma Aldrich (The Netherlands). The fold change induction was normalized to the gene expression level of RPS18 as a house keeping gene.

Supplementary Table 1: List of primers for quantitative real-time PCR

Gene	Forward primer	Reverse primer
α-SMA	CCCCATCTATGAGGGCTATG	CAGTGGCCATCTCATTTTCA
ITGA5	CAACTTCTCCTTGGACCCCC	GTCCTCTATCCGGCTCTTGC
Col1a1	GTACTGGATTGACCCCAACC	CGCCATACTCGAACTGGAAT
CD44	AGGAACCTGCAGAATGTGGA	GTTAAGTGTCCCAGCTCCCT
ABCC1	TTCCCCTGAACATTCTCCCC	CATTCCTCACGGTGATGCTG

BCL2	GTCTGGGAATCGATCTGGAA	AATGCATAAGGCAACGATCC
KRAS	GAGGCCTGCTGAAAATGACTG	ATTACTACTTGCTTCCTGTAGG
MMP-2	AGGAGGAGAAGGCTGTGTTC	CTCCAGTTAAAGGCGGCATC
MMP-9	TCTTCCCTGGAGACCTGAGA	TTTCGACTCTCCACGCATCT
WNT-1	CCTCCACGAACCTGCTTACA	TCCCCGGATTTTGGCGTATC
CXCL-1	ATGCCAGCCACTGTGATAGA	TCCCCTGCCTTCACAATGAT
CSF-3	TAGCGGCCTTTTCCTCTACC	CAGTTCTTCCATCTGCTGCC
IL-1β	CAGAAGTACCTGAGCTCGCC	AGATTCGTAGCTGGATGCCG
RPS18	TGAGGTGGAACGTGTGATCA	CCTCTATGGGCCCGAATCTT

Supplementary Table 2: List of primary and secondary antibodies

Antibody	**Source**	**Dilution**
Mouse monoclonal β-actin	Thermo Fisher Scientific	1:5000
Rat polyclonal CD31	Southern Biotech	1:50
Mouse monoclonal YAP antibody	Santa Cruz	1:50
CXCL-12 polyclonal Antibody	Santa Cruz	1:50
Anti-STUB1/CHIP antibody	Abcam	1:250
IL-6 Polyclonal Antibody	Thermo Fisher Scientific	1:100
mouse monoclonal anti-HIF-1 alpha	R&D Systems	1:100
Anti-collagen type 1	Southern Biotech	1:250
Alexa Flour TM488 donkey anti-mouse	Thermo Fisher Scientific	1:100
Alexa Flour TM549 donkey anti-rabbit	Thermo Fisher Scientific	1:100
Alexa Flour TM488 donkey anti-rabbit	Thermo Fisher Scientific	1:100
Alexa Flour TM488 donkey anti-goat	Thermo Fisher Scientific	1:100
HRP-conjugated goat anti-rabbit IgG	DAKO	1:2000
HRP-conjugated goat anti-mouse IgG	DAKO	1:2000

AV3-Cy3/IR680 conjugation and HPLC characterization

AV3-Cy3 conjugation: AV3-PEG-NH_2 (0.1mg) was dissolved in 5µl of DMSO and added to 40ul of PBS. Cy3-NHS (0.2mg) was dissolved in 10µl of anhydrous DMSO and added to the peptidomimetic solution, then pH was adjusted to 7.4. For, AV3-IR680 conjugation, AV3-PEG-NH_2 (0.29mg) was dissolved in 10µl of DMSO and added to 75µl of 10x PBS (pH adjusted to 7.4). IR680 NHS (0.25mg) was dissolved in 10µl of anhydrous DMSO and added dropwise to the peptidomimetic solution and reacted at 4˚C for 16 h.

The resulting mixture solutions were purified by 2kDa dialysis cassette and confirmed the conjugate construct using HPLC. The HPLC method used an Ultimate® 3000 uHPLC (Thermo Scientific) equipped with a UV/vis detector (λ = 280/555nm) and C18 UPLC column.

Liposomes preparation

Lipids and dyes were purchased commercially as follows: 1,2-dimyristoyl-sn-glycero-3-phosphocholine (DMPC, Sigma Aldrich), Cholesterol (Sigma Aldrich), 1,2-distearoyl-sn-glycero-3-phosphoethanolamine-N-[carboxy(polyethylene glycol)-2000] (DSPE-PEG-COOH, Avanti Polar Lipids, Alabama, USA), 1,2-distearoyl-sn-glycero-3-phosphoethanolamine-N-[(polyethylene glycol)-2000] (DSPE-PEG, Sigma Aldrich), 1,2-distearoyl-sn-glycero-3-phosphoethanolamine-N-[carboxy(polyethylene glycol)-2000] (DSPE-PEG-NH2, Sigma Aldrich), IRDye®, CW800 NHS Ester (LI-COR, Lincoln, NE, USA), 1,1'-Dioctadecyl-3,3,3',3'-Tetramethylindocarbocyanine Perchlorate ('DiI'; DiIC18(3), Thermo Fischer Scientific).

Liposomes were prepared based on the ethanol injection technique [49]. For *in vitro* uptake studies, lipid solutions of DMPC: Cholesterol: DSPE-PEG: DSPE-PEG-COOH: DiI at a molar ratio of 6.5: 3: 0.45: 0.05: 0.02 were used. For *in vivo* studies, DSPE-PEG-NH2 lipid was modified with CW800 NHS in the presence of 0.004% triethanolamine, the reaction mixture was reacted at room temperature for 2 h. The lipid solutions of DMPC: Cholesterol: DSPE-PEG: DSPE-PEG-COOH at the molar ratio of 6.5: 3: 0.422: 0.05 were added to the modified DSPE-PEG-CW800 lipid. For all liposomal formulations, the lipid mixtures were dissolved in ethanol at 30˚C. Crude liposomes were formed by mixing the warm lipid mixture with PBS (1:10, vol: vol) under constant vortex. The crude liposomal size was reduced by repeated extrusion through a polycarbonate membrane (Whatman, UK), pore size 200nm, 100nm, using an Avastin Lipofast extruder. After preparation, liposomes were purified

using a PD10 column (GE healthcare). The liposome size (in PBS) and zeta potential (in 10mM KCl) were measured using Zetasizer Nano ZS (Malvern, UK). The liposomes were stored at 4˚C

AV3 peptide conjugation to liposomes

Liposomes were purified, and their buffer was exchanged to MES buffer (pH=6.3) using PD-10 columns (GE Healthcare, Little Chalfont, UK). Next, the COOH group on DSPE-PEG-COOH was activated using a 50x molar excess of N-hydroxysulfosuccinimide (Sulfo-NHS, Sigma Aldrich) and 1-ethyl-3-(3-dimethyl aminopropyl)carbodiimide hydrochloride (EDC, Sigma Aldrich) for 45 mins at RT on a roller. Next, the buffer was changed to 10x PBS (pH=7.4), and excess of EDC and NHS was removed using a PD-10 column (GE Healthcare). Afterward, AV3-NH2 was added to the liposomes using 2,5x molar excess of peptides compared to DSPE-PEG-COOH and reacted overnight at 4˚C. To block unreacted sulfo-NHS esters, the liposomes were incubated with 12,5x molar excess of glycine compared to DSPE-PEG-COOH and reacted for 1 h at RT. Subsequently, unreacted peptides and glycine were removed by 3 times washing with 30 kDa Amicon columns (Sigma Aldrich).

In vitro cellular binding of nanoparticles

hPSC were seeded in a density 2 x 10^4 cells per will in 12 well-plate and activated with 5 ng/ml human recombinant TGF-β1 (myCAF) or 1 ng/ml of IL-1α (iCAF). Cells were PBS-washed and incubated with detaching buffer containing 0.5% BSA and 5 mM of Ethylenediaminetetraacetic acid (EDTA; Sigma-Aldrich) in PBS for 15. Then, cells were washed and incubated with blocking buffer, composed of 0.9% sodium azide, 0.5% BSA and 2 mM EDTA in PBS for 30 mins. Later, cells were incubated with DiI-labelled nanoparticles in blocking buffer for 60 mins. Next, cells were washed by the blocking buffer and samples were run on MACSQuant® flow cytometer (Miltenyi Biotec. Bergisch Gladbach, Germany).

3D heterospheroid model

Heterospheroids were generated by co-culturing PANC-1 and PANC-1 + hPSC (1:5), respectively in a balanced 1:1 (v/v) mixture of complete DMEM and stellate cell medium. Cells were seeded in a density of 6 x 10^3 cells per well in 96-well round bottom plates coated with 1% Pluronic F-127 (Sigma Aldrich). The growth of

spheroids were followed using an inverted microscope after the treatment with YL-109 and/or gemcitabine. To examine the effect on gene expression, spheroids were isolated and processed for the gene expression analyses using qPCR. CTglo assay was performed to determine %ATP.

Supplementary Figures

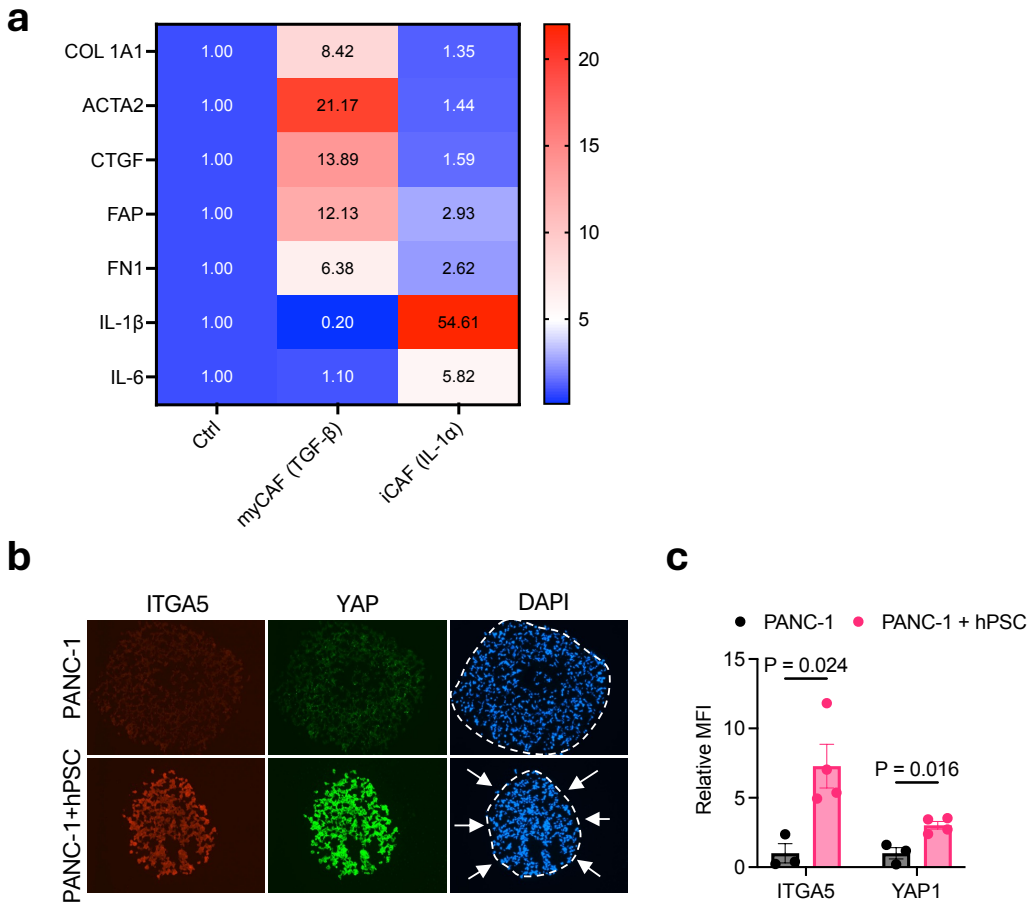

Supplementary Figure 1. (**a**) Heatmap showing mRNA expression for different markers related to myCAF and iCAF upon treatment with TGF-β1 and IL-1α in human pancreatic stellate cells. Data represent the mean for two independent experiments. (**b**) Representative immunofluorescence microscopic images showing the expression of ITGA5 and YAP in 3D heterospheroids (PANC-1+hPSC) compared to 3D homospheroids (PANC-1). Quantitative analyses of the staining show a significant increase in the expression. Statistical analysis was performed using unpaired student's t test for multiple comparison.

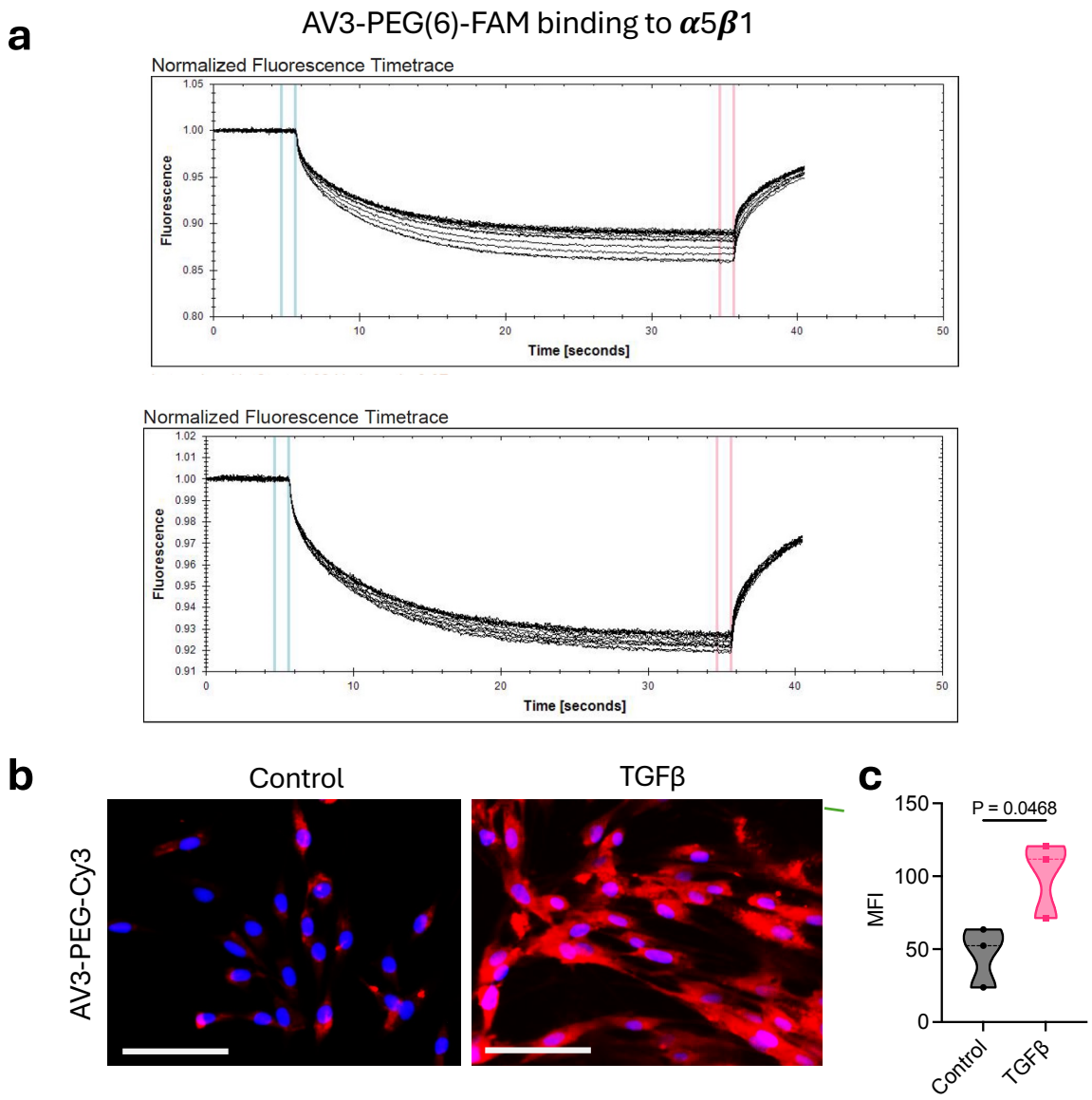

Supplementary Figure 2. (**a**) Fluorescence time traces for AV3-PEG(6)-FAM binding to human recombinant α5β1 (upper) and α4β1 (lower) receptors using microscale thermophoresis analysis. (**b**) Fluorescence microscopic images showing binding of AV3-PEG(6)-cy3 (10 μM) to hPSC with/without the activation with TGFβ1. Scale bar 100 μm. (**c**) violin graphs show the quantitation data with flow cytometry at 0.5 μM concentration.

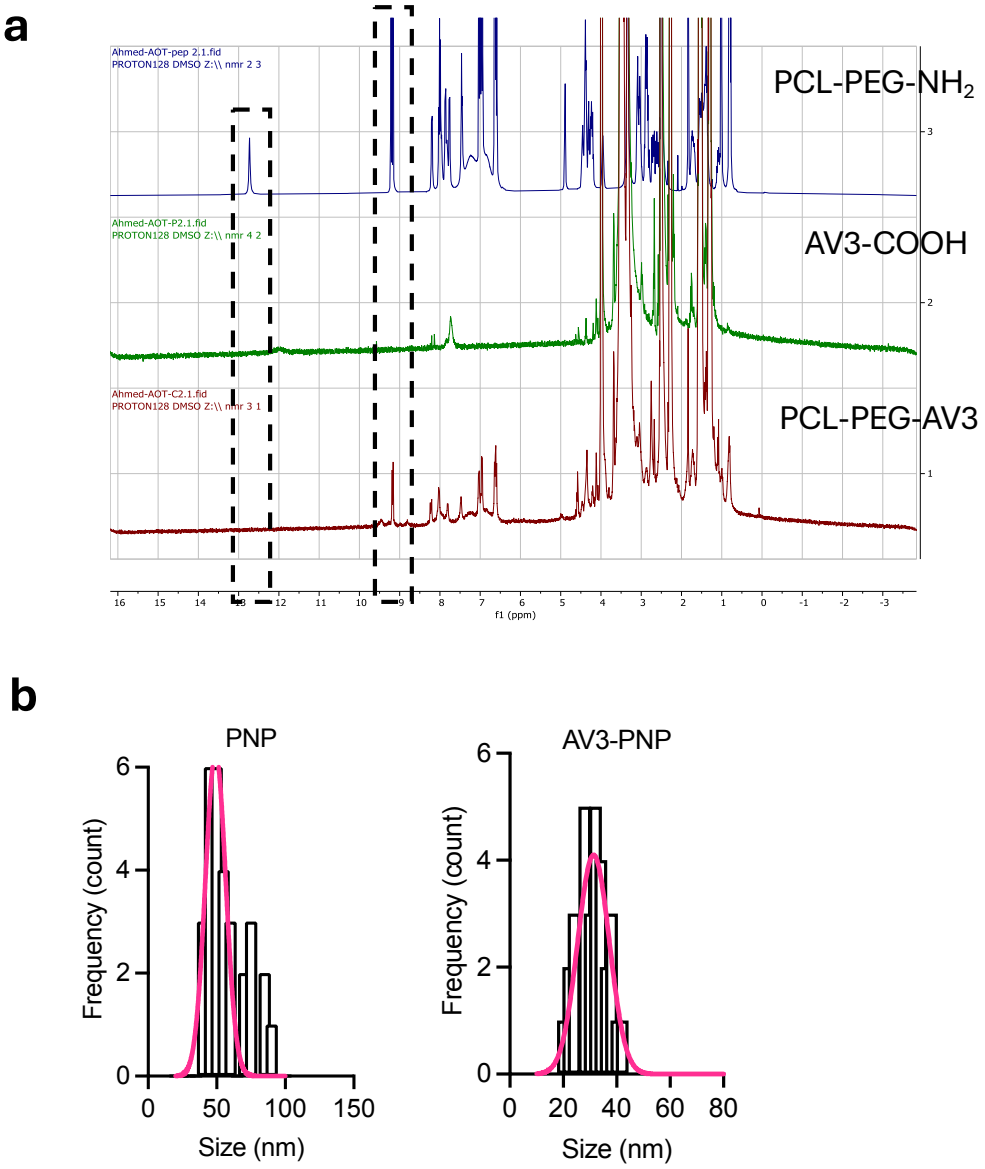

135

136 **Supplementary Figure 3. Characterization of AV3-functionalized PCL-PEG and AV3 nanoparticles.** (A)

137 Proton NMR spectra of PCL-PEG-NH2 (blue), AV3 (green) and the PCL-PEG-AV3 conjugate (red). Dotted

138 box indicates free -COOH proton peak.

139

140

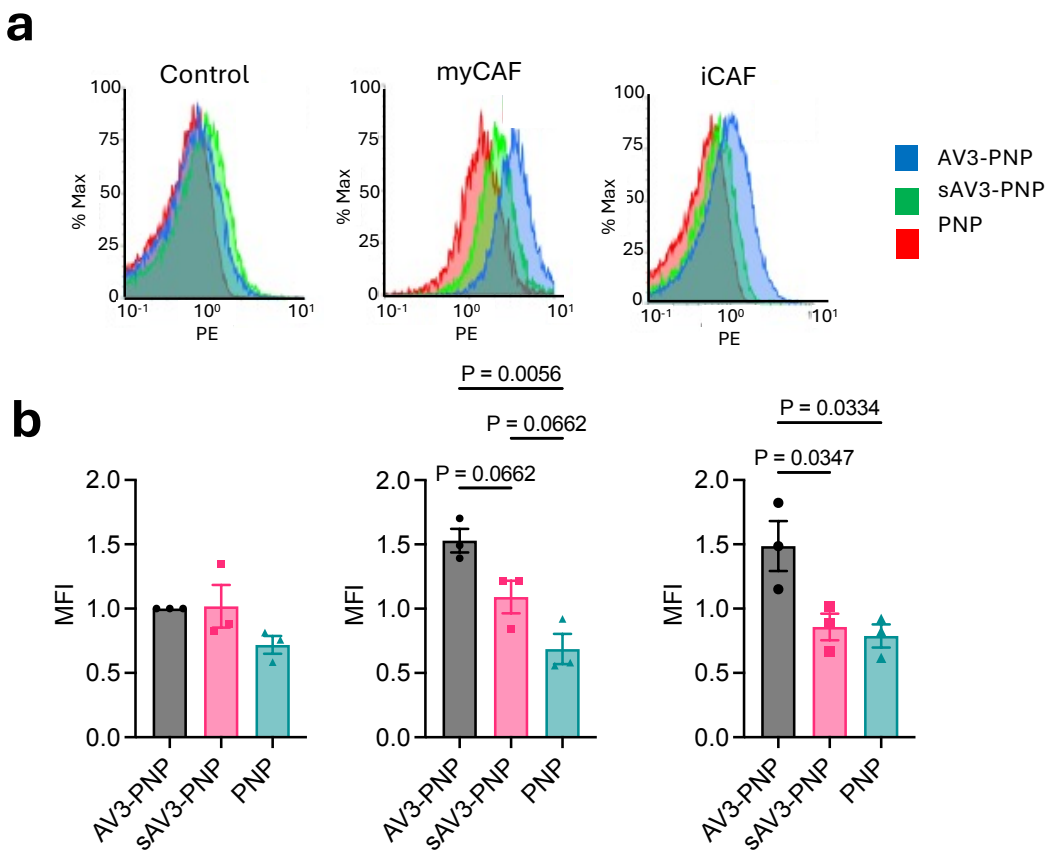

Supplementary Figure 4. (**a**) Flow cytometry histograms and (**b**) quantitative analysis for the binding of fluorescence dye-labelled nanoparticles to quiescent hPSC, myCAF (TGF-β-activated) and iCAF (IL-1α-activated). Data represent mean ±SEM (*n=3*). One-Way ANOVA with multiple comparison corrected by Holm Sidak test.

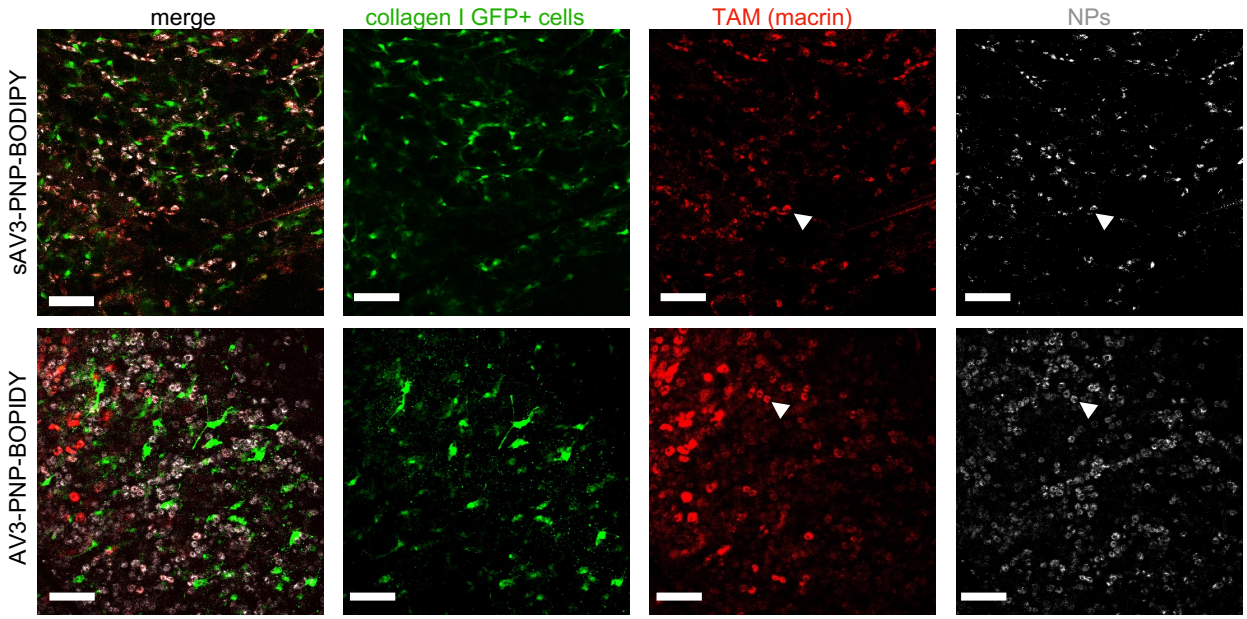

Supplementary Figure 5. Multi-colour fluorescence microscopic images showing the co-localization of AV3-PNP-BODIPY and sAV3-PNP-BODIPY with CAFs (EGFP+ green cells) and TAMs (Macrin+ red cells) in KPC tumour bearing transgenic collagen-1α1-EGFP+ mice at t=24 h after the intravenous injection. Scale bar: 100 μm. (**b**) Scatter graphs and histograms for the flow cytometry analysis showing the gating schemes and differences for the uptake of RhB-labelled different nanoparticles (AV3-PNP, sAV3-PNP, PNP) by myCAF, iCAF and TAMs in vivo.

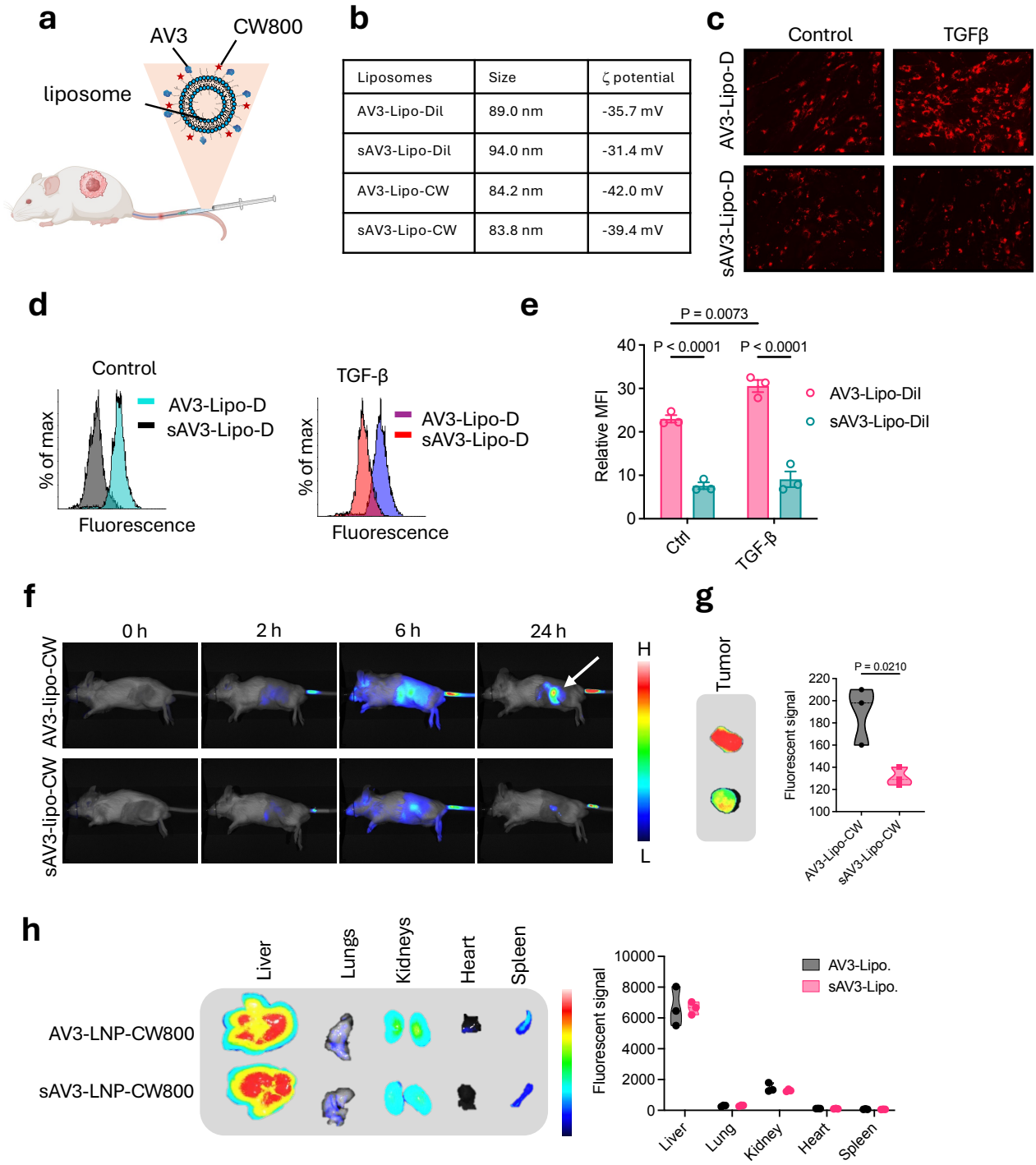

158

159 **Supplementary Figure 6. (a)** Schematic illustration showing AV3-conjugated liposomes modified with

160 CW800 NIR dye or encapsulating DiI dye. (**b**) Size and zeta potential of typical liposomal formulations. (**c**)

161 Fluorescence microscopic images and (**d, e**) showing the uptake of AV3-Lipo-DiI and sAV3-Lipo-DiI in hPSC

162 with/without TGF-β1 treatment. Mean ± s.e.m. n=3. Two-Way ANOVA corrected with Holm Sidak method.

163 (**f**) In vivo NIR imaging of mice injected with AV3 or sAV3 conjugated liposomes labelled with CW800 NIR

dye in co-injection PDAC model until t=24h. (**g**) Representative NIR images and quantitation of the isolated tumours. Data present n=3 mice per group. Statistical analysis was performed using two-sided unpaired t test. (**h**) Representative NIR images and quantitation of different organs from n=3 mice per group. Data present n=3 mice per group. Statistical analysis was performed using multiple comparison two-sided unpaired t test. No significance was found.

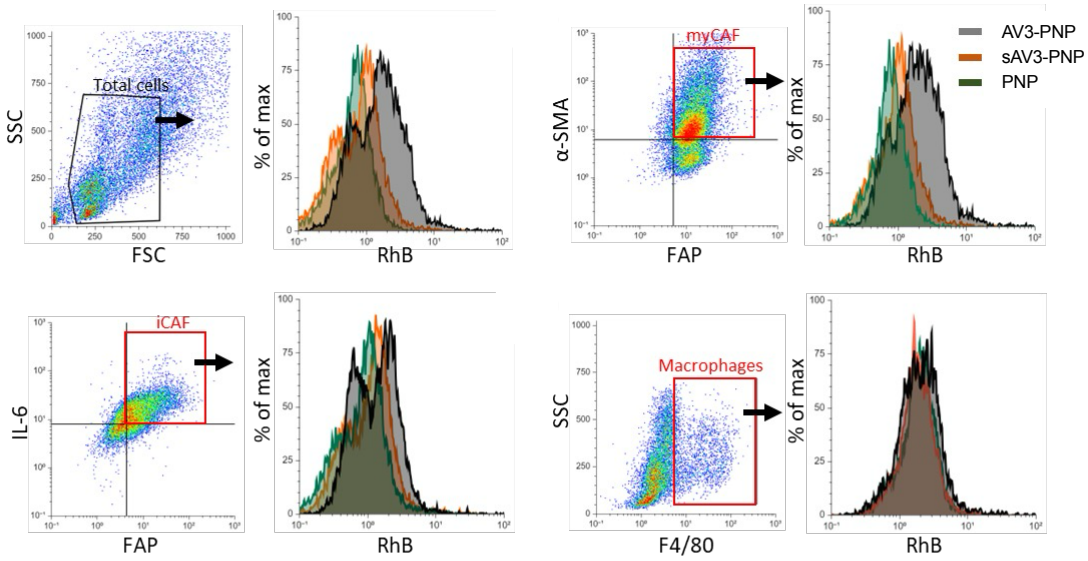

171

172

173 **Supplementary Figure 7.** Scatter graphs and histograms for the flow cytometry analysis showing the gating
174 schemes and differences for the uptake of RhB-labelled different nanoparticles (AV3-PNP, sAV3-PNP, PNP)
175 by myCAF, iCAF and TAMs in vivo.

176

177

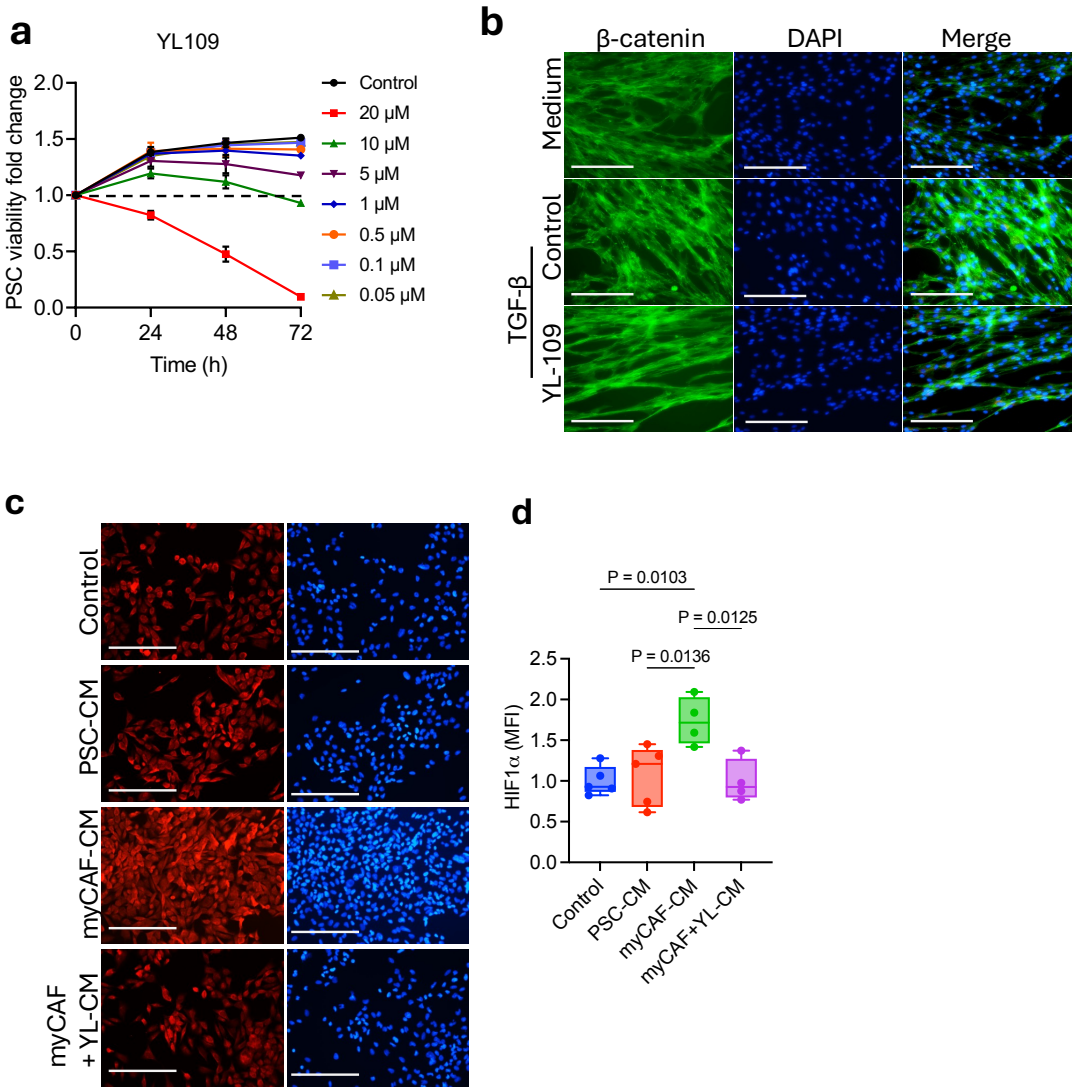

178

179

180 **Supplementary Figure 8. YL109 inhibits TGF-β-induced overexpression of beta catenin.** (**a**)
181 Representative fluorescence microscopy images and (**b**) quantification of β-catenin expression by TGF-β-
182 activated hPSC. Scale bar: 200 μm. Graphical data represent mean ± s.e.m. (n=3). (**c, d**) Immunofluorescence
183 staining and quantitation of HIF-1α in PANC-1 cells treated with conditioned media collected from either hPSC,
184 myCAFs (TGF-β treated) or myCAF-treated with YL-109. Blue colour represents DAPI staining in nuclei.
185 Scale bar: 100 μm.

186

187

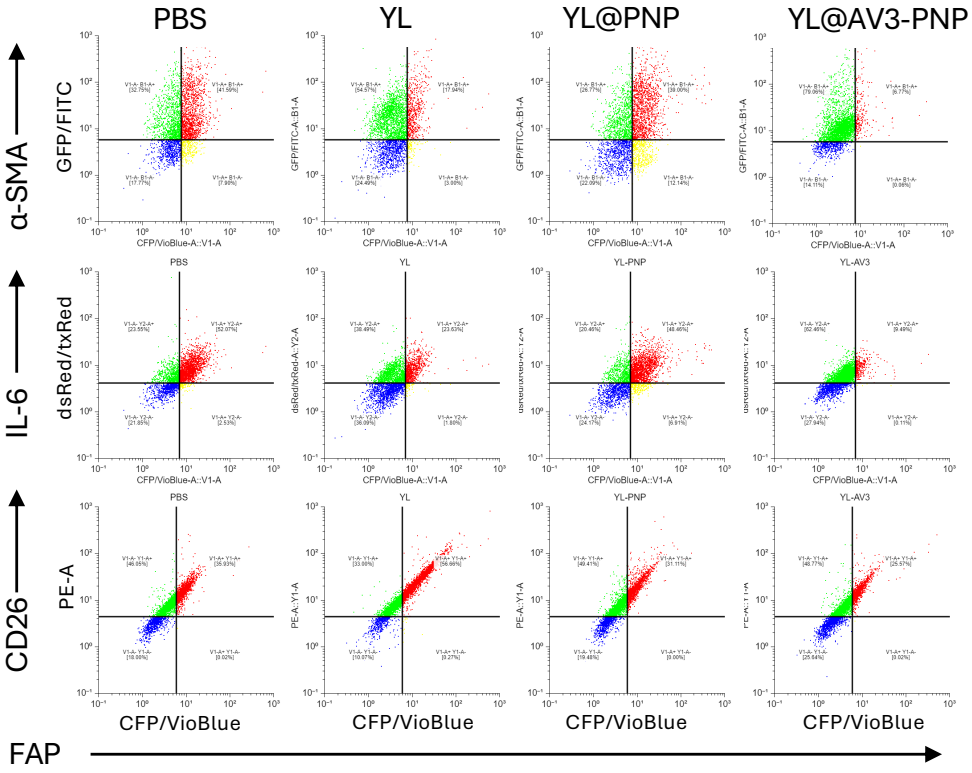

Supplementary Figure 9. Scatter graphs showing the effect of different treatments on the cellular phenotype of CAFs including myCAF (FAP+α-SMA+), iCAF (FAP+IL-6+ or FAP+CD26+).

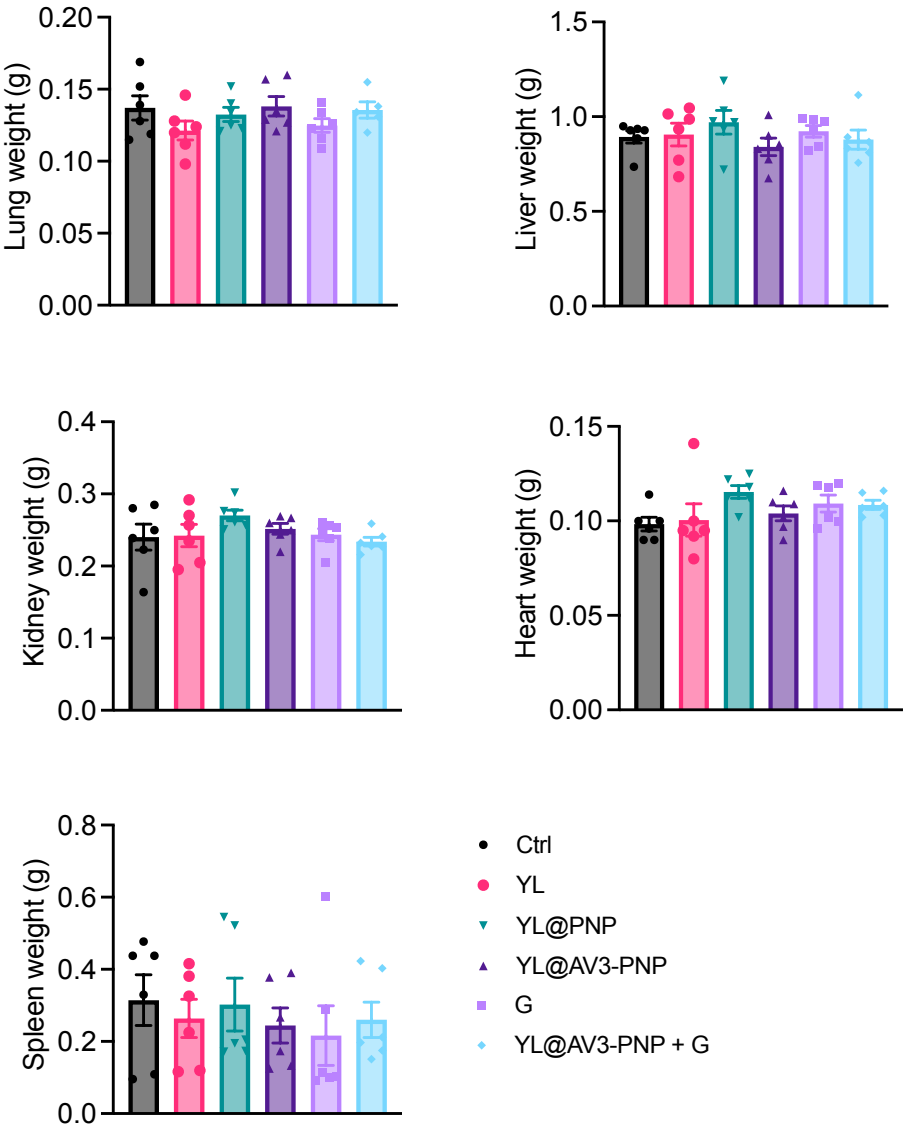

Supplementary Figure 10. Organ weight after different treatments in the KPC tumour model. Mice were treated with either PBS (Ctrl), YL-109 (YL; 5 mg/kg/d, i.p., t.i.w.), YL@PNP (equiv. 5 mg/kg/d, i.v., t.i.w.), YL@AV3-PNP (equiv. 5 mg/kg/d, i.v., t.i.w.), gemcitabine (G; i.p. 50 mg/kg/d, b.i.w.) or YL@AV3-PNP + G. Graphical data represent mean ± s.e.m.

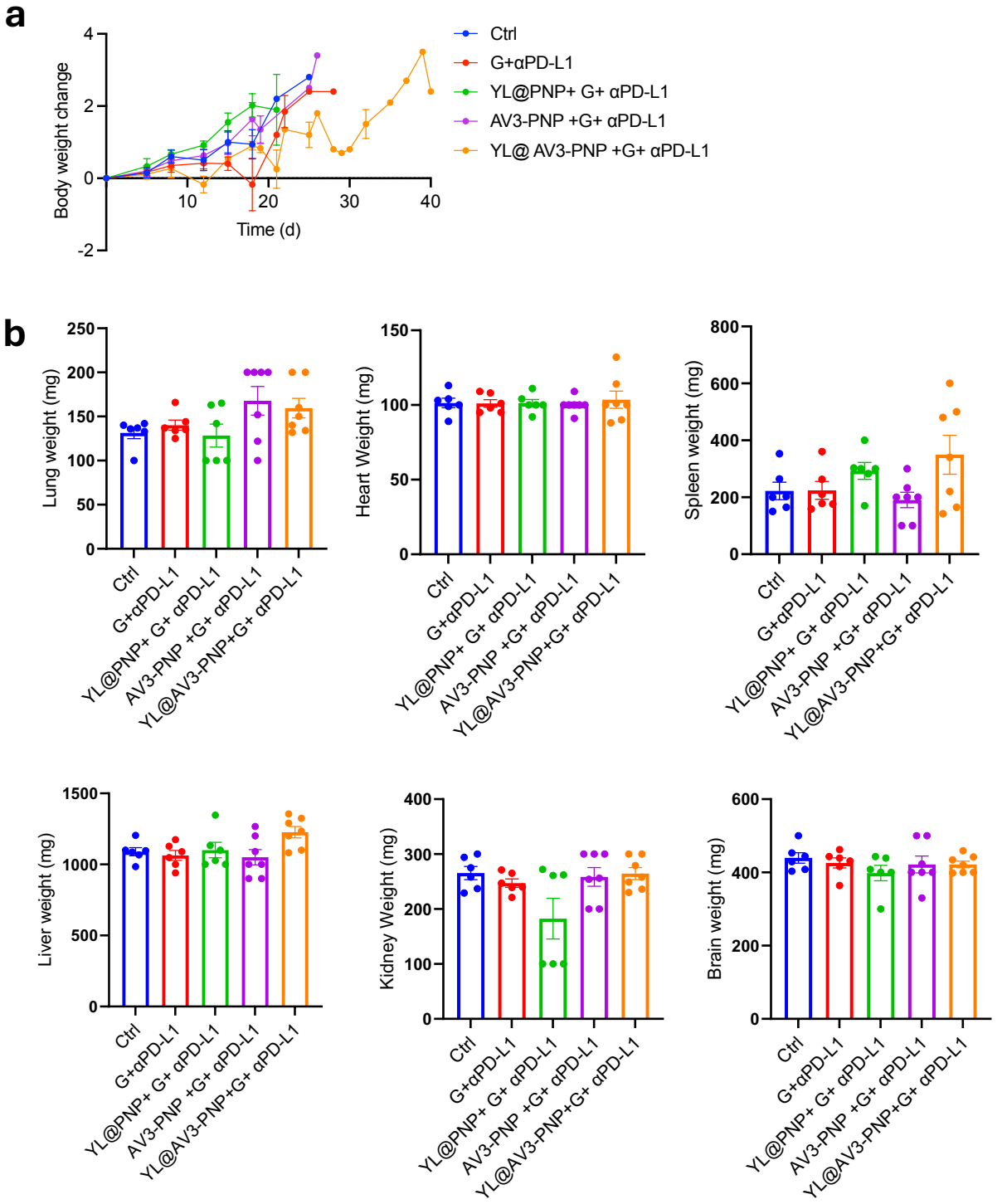

Supplementary Figure 11. Effect of different treatments on the body weight (**a**) and organ weights (**b**) in KPC mouse model. Mice were treated with either PBS (Ctrl), gemcitabine (G; 50 mg/kg/d, i.p., b.i.w.) and αPD-L1 (200 μg/mouse/d, b.i.w.) and combination with YL@PNP, AV3-PNP or YL@AV3-PNP. YL in all formulations was 10 mg/kg/d, i.v., b.i.w. Graphical data represent mean ± s.e.m.